NASA TECHNICAL NOTE

NASA TN D-4444

NASA TN D-4444

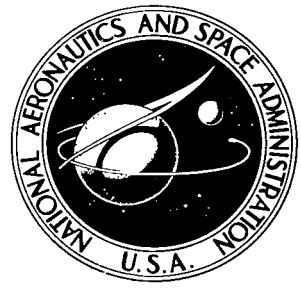

TEXTURE STRENGTHENING AND FRACTURE TOUGHNESS OF TITANIUM ALLOY SHEET AT ROOM AND CRYOGENIC TEMPERATURES

by Timothy L. Sullivan

Lewis Research Center

Cleveland, Ohio

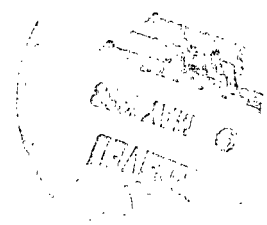

NATIONAL AERONAUTICS AND SPACE ADMINISTRATION • WASHINGTON, D. C. • MAY 1968

TEXTURE STRENGTHENING AND FRACTURE TOUGHNESS OF TITANIUM ALLOY SHEET AT ROOM AND CRYOGENIC TEMPERATURES

By Timothy L. Sullivan

Lewis Research Center
Cleveland, Ohio

NATIONAL AERONAUTICS AND SPACE ADMINISTRATION

For sale by the Clearinghouse for Federal Scientific and Technical Information
Springfield, Virginia 22151 – CFSTI price $3.00

TEXTURE STRENGTHENING AND FRACTURE TOUGHNESS OF TITANIUM ALLOY SHEET AT ROOM AND CRYOGENIC TEMPERATURES

by Timothy L. Sullivan

Lewis Research Center

SUMMARY

Preferred crystallographic orientation or texturing in metallic sheet can, under conditions of biaxial stress, result in strengthening considerably greater than that predicted for an isotropic material. Certain titanium alloys exhibit texturing. After it is rolled into sheet form, titanium alloyed with about 4 percent aluminum gives close to the ideal texture for maximum biaxial strengthening. The commercially available titanium alloy, Ti-5Al-2.5Sn, also exhibits texture strengthening. The effect of texturing on the yield, ultimate, notch, and weld strengths of both Ti-4Al-0.2O and Ti-5Al-2.5Sn extra-low-interstitial (ELI) grade was determined by testing 0.020-inch- (0.051-cm-) thick sheet in uniaxial and 1 to 2 biaxial stress fields at 20°, 77°, and 294° K. The biaxial test specimens were cylinders 6 inches (15.2 cm) in diameter and 18 inches (45.7 cm) long. In addition, plastic Poisson's ratios were determined at the three test temperatures.

The ratio of 1 to 2 biaxial to uniaxial yield strength ranged from 1.36 at 20° K to 1.53 at 294° K for the Ti-4Al-0.2O alloy (room-temperature plastic Poisson's ratio μ_p, 0.845) and from 1.24 at 20° K to 1.37 at 294° K for the Ti-5Al-2.5Sn ELI alloy (room temperature μ_p, 0.732). Substantial increases in ultimate strength were also obtained. Although the Ti-4Al-0.2O alloy had less uniaxial strength than did the Ti-5Al-2.5Sn ELI alloy, its more heavily textured condition generally resulted in greater 1 to 2 biaxial strength. The Ti-4Al-0.2O alloy also exhibited superior biaxial weld strength. Tests of through-cracked cylinders at 20° and 77° K showed the Ti-4Al-0.2O alloy to have greater notch sensitivity. However, for through cracks 0.10 inch (0.25 cm) or less, the 1 to 2 biaxial notch strengths of the two alloys are about equal. The use of plastic Poisson's ratio to predict the increase in biaxial yield strength resulted in good agreement with experimental values.

INTRODUCTION

Certain anisotropy in sheet materials can cause appreciable strengthening under conditions of biaxial stress. The form of anisotropy referred to is called texturing and is characterized by isotropy in the plane of the sheet with considerable anisotropy normal to this plane. For the purely isotropic case, yielding in a 1 to 2 stress field is predicted to occur at 1.15 times the uniaxial yield strength. For textured materials, however, yield strengths 1.5 times uniaxial yield strength or greater have been predicted for the same stress field (ref. 1). Uniaxial studies of texturing in titanium alloys have been made by several investigators (refs. 2 to 4). Sliney, et al. (ref. 5) and Babel, et al. (ref. 6) have experimentally investigated the biaxial strengthening of Ti-5Al-2.5Sn alloy cylindrical pressure vessels at room temperature. This work reports the results of an investigation of biaxial strengthening in an experimental textured titanium alloy, Ti-4Al-0.2O, at temperatures as low as 20° K.

In alpha titanium alloys, maximum strengthening occurs when the basal (0001) planes of the hexagonal close-packed crystals are parallel to the plane of the sheet (fig. 1). In unalloyed titanium sheet, the basal planes are inclined approximately 30° toward the transverse direction. However, certain alloying agents (i.e., alpha stabilizers) inhibit rotation of these planes, and the addition of 3.8 percent aluminum gives close to the ideal texture after rolling (ref. 7). The addition of critical amounts of oxygen (approximately 0.2 percent) and iron (approximately 0.1 percent) increases the strength of the alloy and makes it easier to roll than its commercial counterparts (ref. 8). Because of the potential usefulness of this alloy as a cryogenic propellant tank material, a program was undertaken at Lewis Research Center to determine the strength and fracture toughness of 0.020-inch- (0.051-cm-) thick Ti-4Al-0.2O sheet in both uniaxial and 1 to 2 biaxial stress

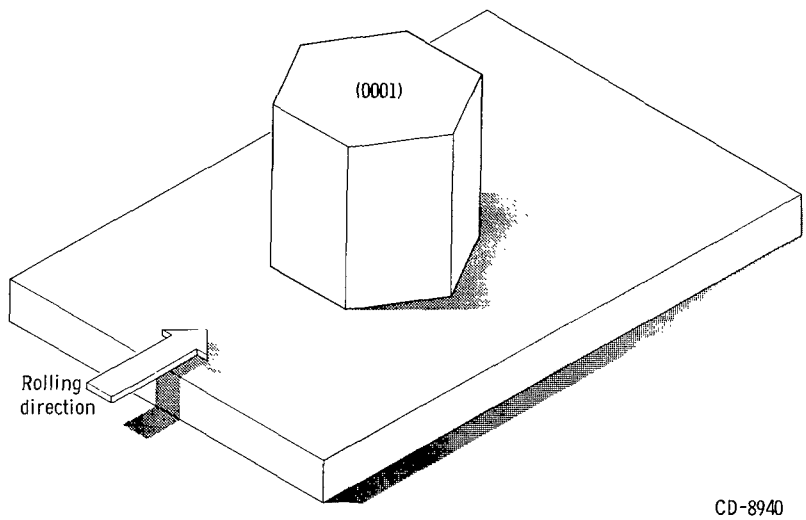

Figure 1. - Ideal orientation of hexagonal close-packed crystal for maximum strengthening in biaxial stress field.

fields. A parallel study was conducted with a commercially available titanium alloy that exhibits texturing, Ti-5Al-2.5Sn extra-low-interstitial (ELI) grade. The results of these studies are compared. In addition, the weld strengths of a limited number of uniaxial and biaxial test specimens were determined.

Uniaxial smooth and notch properties of both alloys were determined at 20°, 77°, and 294° K (-423°, -320°, and 70° F). Smooth biaxial properties were determined from burst tests of 6-inch- (15.2-cm-) diameter cylindrical pressure vessels over the same range of test temperatures. Tests of notched pressure vessels were made at 20° and 77° K. Basal pole figures were obtained for both alloys. The increase in biaxial yield strength (over uniaxial yield strength) is correlated with the plastic Poisson's ratio obtained from a uniaxial tension test.

ANALYTICAL BASIS FOR TEXTURE STRENGTHENING

By applying Hill's theory (ref. 9) for the yielding of anisotropic sheet materials, Backofen, et al. (ref. 1) indicate that for the case of rotational symmetry about the thickness direction (isotropy in the plane of the sheet) the yield criterion becomes

$$\frac{\sigma_x}{\sigma_{ys}} = \left(1 + \alpha^2 - \alpha \frac{2R}{R + 1}\right)^{-1/2} \tag{1}$$

where α is the ratio of the principal stresses in the plane of the sheet σ_y/σ_x, σ_{ys} is the uniaxial yield strength in the plane of the sheet, and R is the ratio of plastic strain in the width direction of the sheet ϵ_w to plastic strain in the thickness direction of the sheet ϵ_t. (These strains can be determined from smooth uniaxial tension tests.) It is assumed in equation (1) that the principal directions of anisotropy correspond with the principal directions of stress. The derivation of this equation is given in appendix A of reference 5.

Because of the difficulty in accurately measuring strain in the thickness direction of thin gage materials, R can be based on a more easily measured quantity, such as strain in the length direction ϵ_l. This can be done if constancy of volume is assumed. If yielding has occurred, $\epsilon_l + \epsilon_w + \epsilon_t = 0$ for small strains. Thus,

$$R = \frac{\epsilon_w}{\epsilon_t} = \frac{\epsilon_w}{-\epsilon_w - \epsilon_l} = \frac{\mu_p}{1 - \mu_p} \tag{2}$$

where μ_p is plastic Poisson's ratio $-\epsilon_w/\epsilon_l$.

EXPERIMENTAL APPARATUS AND PROCEDURE

Test specimens were fabricated from sheet, nominally 0.020 inch (0.051 cm) thick, produced from a single heat for each alloy. The sheet was annealed at 990° K (1325° F) for 4 hours and furnace cooled. The mill analysis provided by the supplier is given in the following table:

Material	Heat	Composition, wt %							
		C	Fe	N	Al	H	O	Sn	Mn
Ti-4Al-0.2O	V-3002	0.023	0.12	0.014	3.8	0.007 to 0.010	0.21	---	------
Ti-5Al-2.5Sn ELI	D-3272	0.022	0.08	0.014	5.1	0.006 to 0.009	0.08	2.5	<0.006

Uniaxial Tests

The specimens used to determine the uniaxial properties of the sheet are shown in figure 2. Finished specimens were stress relieved in the same manner as outlined in the following section for biaxial test specimens. Conventional smooth properties, including 0.2 percent offset yield strength and plastic Poisson's ratio, were obtained by using the specimen shown in figure 2(a). Weld specimens were of this type and had their weld beads normal to the loading axis. Weld beads were not ground flush with the

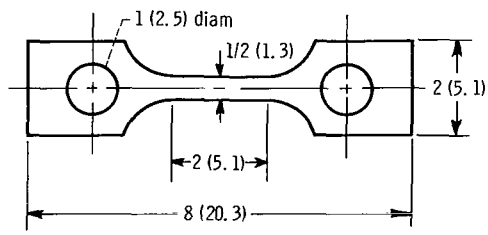

(a) Smooth specimen.

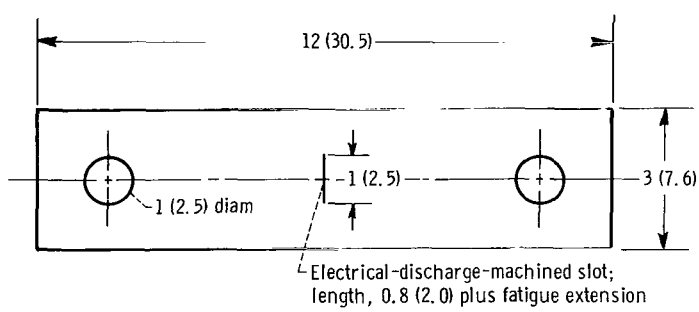

(b) Center-cracked specimen.

Figure 2. - Sheet specimens. (All dimensions are in inches (cm).)

parent metal so that they would closely model the fabrication of component hardware. Notch strength (based on initial crack length) and fracture toughness (based on critical crack length) were determined by using the specimen shown in figure 2(b). Cryogenic test temperatures were obtained by immersing the specimens in liquid nitrogen or liquid hydrogen.

The NASA continuity gage (ref. 10) was used to measure the slow crack growth which took place prior to catastrophic failure. At 20° K, the transition between slow and rapid crack growth was abrupt, and the critical crack length was readily obtainable directly from the gage output. At 77° K, however, the transition was gradual, and a crack velocity of 0.1 inch (0.25 cm) per second was arbitrarily selected to define the critical crack length. Because the crack velocity selected is relatively slow, the critical crack lengths used to calculate fracture toughness gave conservative results.

Plastic Poisson's ratios were obtained by use of high-elongation copper-nickel foil strain gages on the test section of tensile specimens. One gage was mounted parallel to the direction of loading on one side of the specimen, while a second gage was mounted transverse to the direction of loading on the other side of the specimen and directly behind the first gage. This arrangement allowed strain measurement in both directions at essentially the same location. Strain differences from one surface to the other due to bending would not be expected from the thin sheet used in this investigation. The output of the gages was used to drive an X-Y recorder. The specimen was loaded in tension until yielding had occurred. The load was then held constant as the strain continued to increase until the end of the recorder chart travel was reached (about 2 percent strain). This procedure restricted the strain ratio to purely plastic (nonrecoverable) strain

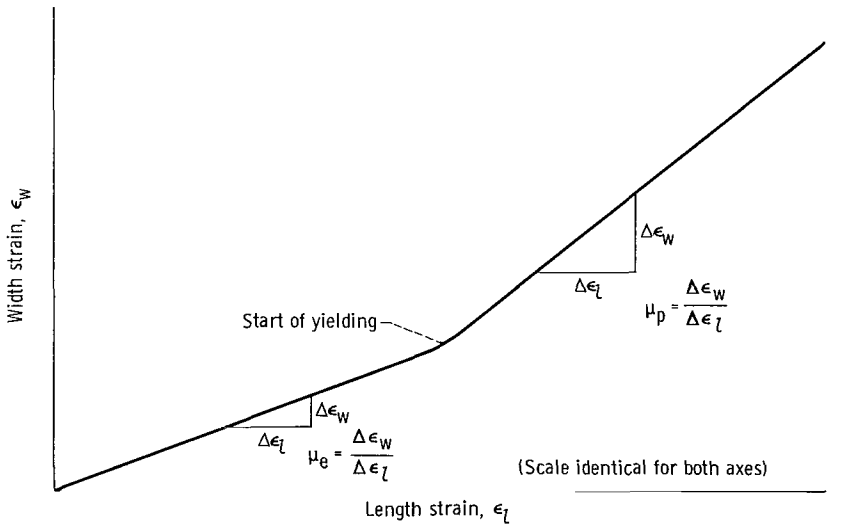

Figure 3. - Record of typical width strain as function of length strain for Ti-4Al-0.20 sheet at room temperature. Plastic Poisson's ratio μ_p, 0.840; elastic Poisson's ratio μ_e, 0.395.

components in accordance with the assumption of volume constancy. The slope of the curve of ϵ_w against ϵ_l after yielding occurred was taken as the plastic Poisson's ratio. A typical record of ϵ_w as a function of ϵ_l is shown in figure 3.

Biaxial Tests

Cylindrical pressure vessels 6 inches (15.2 cm) in diameter and 18 inches (45.7 cm) long were fabricated by using a single longitudinal butt weld. The sheet was oriented so that its rolling direction corresponded to the hoop direction of the cylinder. Welding was performed in an argon-inerted chamber with a tungsten electrode. No filler material was added. After fabrication, cylinders were stress relieved in vacuum and furnace cooled. The stress relief schedules were 1 hour at 811° K (1000° F) for the Ti-4Al-0.2O alloy and 2 hours at 867° K (1100° F) for the Ti-5Al-2.5Sn ELI alloy.

Cracks were produced in cylinders by electrical discharge machining longitudinal slots through the cylinder walls followed by low-stress fatiguing to obtain sharp cracks at the slot ends. An internal patch (ref. 11) was taped over the crack for pressurizing to failure.

Welds were reinforced to preclude weld failures in cylinders used to determine parent-material biaxial yield and ultimate strengths. This reinforcing was done by applying internal and external overlays of commercially pure titanium strip to the weld. The strips were 0.004-inch (0.010 cm) thick and approximately 2 inches (5.1 cm) wide. For room-temperature tests, an epoxy-nylon adhesive was used to bond the strips to the cylinders. For tests at 20° and 77° K a polyester adhesive was used. This adhesive had shown good strength at cryogenic temperatures in lap shear tests. End closure was obtained by sealing the cylinder ends in heads filled with a low-melting-point alloy (ref. 11).

Strippable-backed nickel-chromium foil strain gages were applied to all uncracked cylinders. An epoxy adhesive was used in mounting the gages for room-temperature tests, and the polyester adhesive referred to previously was used for cryogenic tests. One longitudinal gage and one hoop gage were applied 180° from the weld and midway from the ends on the cylinders tested to determine weld strength. For tests to determine the yield and ultimate strengths of the parent tank material, pairs of hoop and longitudinal gages were applied $\pm 90^{\circ}$ and 180° from the weld (fig. 4). An additional hoop gage was applied at one of the 90° stations; the signal from this gage was applied to one axis of an X-Y recorder in order to obtain a continuous record of strain as a function of pressure. The pressure and remaining strain-gage signals were read out incrementally on a multichannel digital strain recorder.

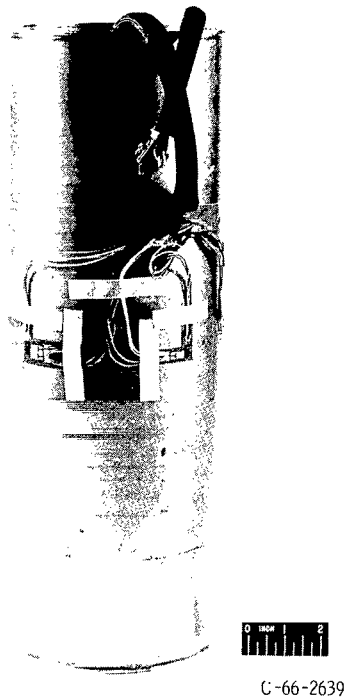

C-66-2639

Figure 4. - Biaxial test specimen.

The cylinders were pressurized to failure by applying helium pressure to liquid hydrogen, liquid nitrogen, or tap water, for tests at 20°, 77°, and 294° K, respectively. For the cryogenic tests, the cylinders were placed in a cryostat and both filled and surrounded with the appropriate cryogen.

In the linear stress-strain range, pressurization of the unflawed cylinders was interrupted at each 100-psi (59-N/cm^2) pressure increment to allow recording of strain-gage data. Pressure readings obtained from strain-gage-type pressure transducers were printed out before and after each pair of hoop and longitudinal strain-gage readings. When a pressure of approximately 80 percent of the anticipated burst pressure was achieved, the strain recorder was made to print data at a rate of 4 channels per second, and the cylinder was pressurized continuously to failure. This procedure provided strain data in the nonlinear stress-strain range at each station at about 10-psi (7-N/cm^2) increments in pressure. Cracked cylinders were pressurized continuously to failure at a rate which ranged from 100 to 200 psi (69 to 138 N/cm^2) per minute. The pressure at which burst occurred was recorded. Accurate pressure readings were assured by calibrating the transducers with a high-accuracy (within 3 psi or 2 N/cm^2) pressure gage before each test. Burst pressures ranged from 120 to 1850 psi (83 to 1276 N/cm^2).

Hoop stress σ was calculated from the pressure p by using the relation $\sigma = pr/t$, where r is the cylinder radius and t is the wall thickness. Failure strengths

were computed from the burst pressure. Yield strengths were obtained by using the 0.2-percent-offset method.

RESULTS AND DISCUSSION

Characterization of Texturing

There are a number of ways to measure the amount of texturing in sheet material, including the following:

(1) The strain ratio parameter R

(2) The ratio of the uniaxial yield strength in the thickness direction to that in the plane of the sheet

However, in thin sheet it is difficult to make accurate measurements in the thickness direction. Because texturing is associated with the orientation of crystals, use of X-ray diffraction methods to determine the crystallographic orientation yields a quantitative indication of the amount of texturing. In this case, the information is plotted on special contour graphs, known as "pole figures", which reveal the nature of the orientation texture (ref. 12). For hexagonal metals a sufficiently accurate representation of the texture is obtained by plotting a pole figure for the basal plane. It is not clear, however, how the pole figure can be used to predict biaxial strengthening quantitatively.

Basal pole figures were obtained for both alloys and are shown in figure 5. Contours of 0, 50, and 90 percent intensity (indicating the density of poles) are shown. For the Ti-5Al-2.5Sn ELI alloy (fig. 5(b)), the contours were nearly circular (within $\pm 2^{\circ}$), and for simplicity they were drawn as circles. A clear comparison of the two pole figures cannot be made. At pole densities of 50 percent and less, the Ti-4Al-0.2O sheet appears more highly textured. On the other hand, the 90-percent-pole-density contour for the Ti-5Al-2.5Sn ELI sheet indicates a higher degree of texture for this alloy. As is shown in the section Biaxial Properties, however, the Ti-4Al-0.2O sheet exhibits greater biaxial strengthening.

Equation (2) shows the relation between plastic Poisson's ratio μ_p and the strain-ratio parameter R when constancy of volume is assumed. Combining equations (1) and (2) results in the following criterion for yielding

$$\frac{\sigma_x}{\sigma_{ys}} = \left(1 + \alpha^2 - 2\alpha\mu_p\right)^{-1/2} \tag{3}$$

Equation (3) indicates that μ_p can quantitatively characterize texturing in a material and can be used to predict biaxial strengthening. It should be noted that while for an

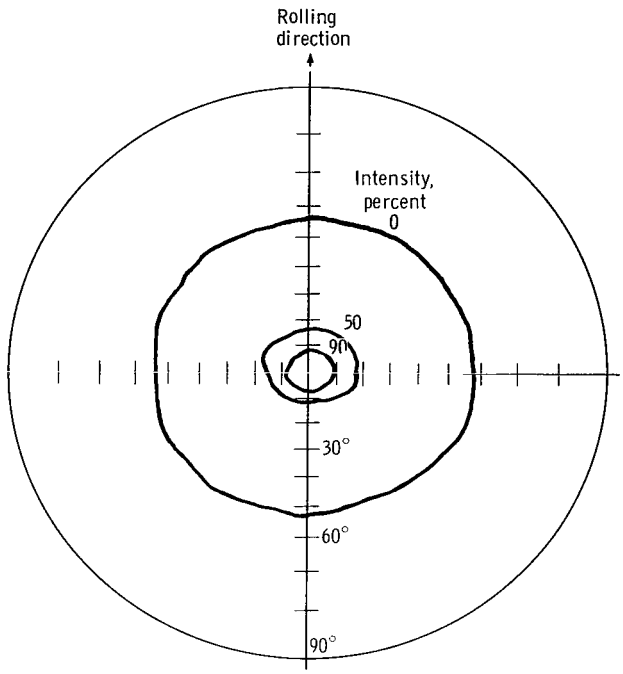

(a) Ti-4Al-0.2O alloy.

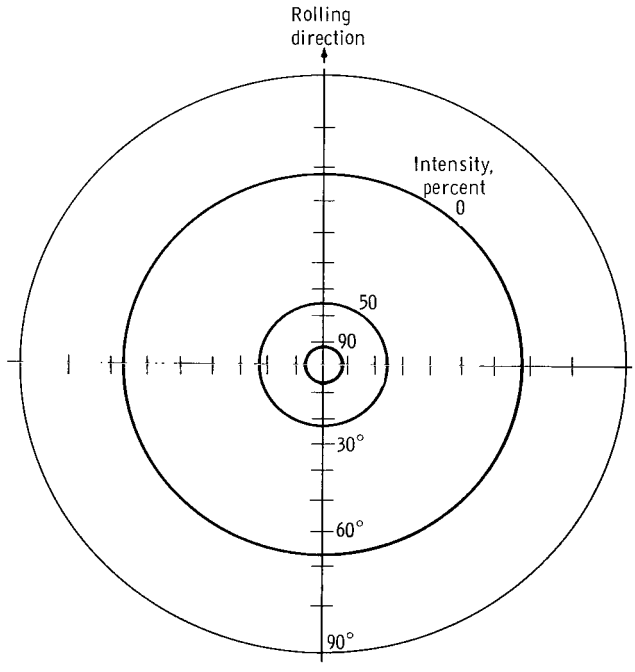

(b) Ti-5Al-2.5Sn ELI alloy.

Figure 5. - Pole figure.

isotropic material $\mu_p = 0.5$, for a textured material μ_p can exceed 0.5 and attain a value as high as 1.0. The reason for this is that a textured sheet when subjected to tension stress exhibits a great resistance to thinning. To maintain constant volume requires greater width contraction than obtained with an isotropic material.

Uniaxial Properties

Average smooth and notch properties for both alloys are plotted as a function of test temperature in figure 6. Specimens were tested with the loading direction both parallel (longitudinal specimen) and normal (transverse specimen) to the rolling direction. At least three specimens were tested for each condition. Individual results are tabulated in tables I and II for smooth and notch specimen tests, respectively. The modulus of elasticity and the elongation in 2 inches (5.1 cm), where measured, are included in table I. For both alloys, only slight differences were found between the longitudinal and transverse yield strengths and the longitudinal and transverse ultimate strengths, which indicates that, at least for these properties, the materials were essentially isotropic in the plane of the sheet. The Ti-5Al-2.5Sn ELI alloy exhibited greater smooth uniaxial strength at all three test temperatures. The difference ranged from about 10 percent at room temperature to about 3 percent at 20° K.

Through-the-thickness center-cracked specimens were tested to determine the behavior of the two materials in the presence of a flaw. The Irwin method (ref. 13) was used to calculate fracture toughness. No effort was made to prevent buckling of the crack lips out of the plane of the sheet during testing. A limited number of tests with antibuckling face plates indicated that buckling can reduce the calculated value of toughness by about 8 percent for the Ti-5Al-2.5Sn ELI alloy at 20° K. The error produced by the omission of antibuckling face plates at other temperatures for the Ti-5Al-2.5Sn ELI alloy was not determined, nor was the influence of buckling investigated for the Ti-4Al-0.2O alloy at any temperature. However, since all tests of notched uniaxial specimens reported herein were performed without antibuckling face plates, the notch strength and fracture toughness values for the two alloys investigated are considered comparable, though conservative.

As would be expected for 0.020-inch- (0.051-cm-) thick sheet, all specimen fractures were characterized by full shear fracture surfaces, accompanied by considerable plasticity. A rather complete statement of the effects of sheet thickness on the fracture toughness of Ti-5Al-2.5Sn alloy is presented in reference 14. It is important to recognize that the present results relate only to 0.020-inch- (0.051-cm-) thick material. While comparison of the two alloys investigated is justified on the basis of identical thicknesses, a comparison with the same or other alloys at thicknesses other than 0.020 inch (0.051 cm) is to be avoided.

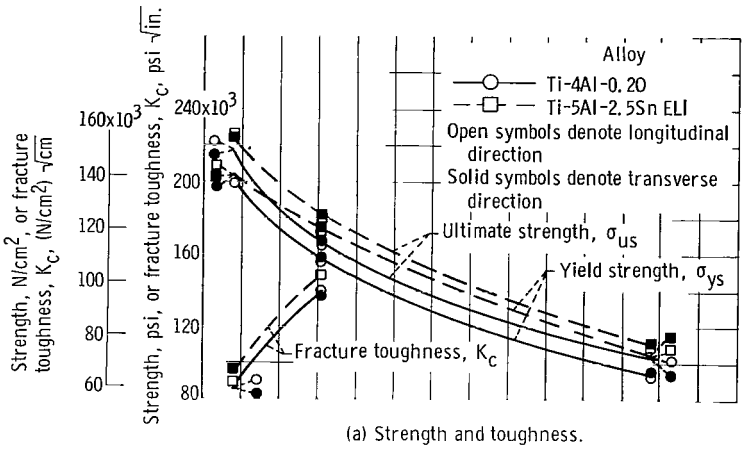

(a) Strength and toughness.

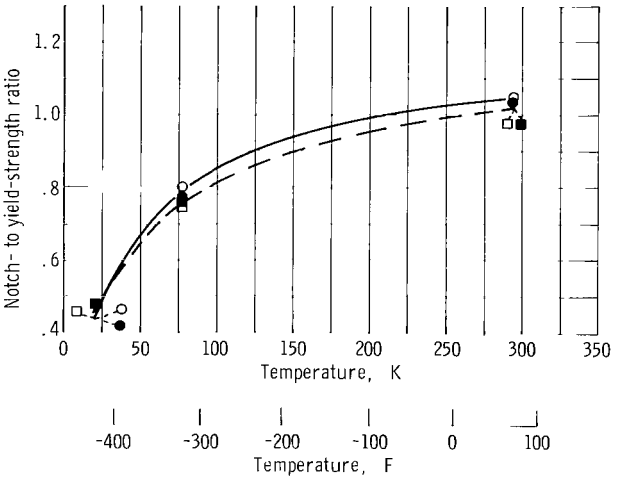

(b) Notch- to yield-strength ratio.

Figure 6. - Average uniaxial properties of Ti-4Al-0.20 and Ti-5Al-2.5Sn ELI sheet as function of test temperature.

As figure 6 shows, the difference in smooth and notch properties between the two alloys was slight. Additionally, directionality effects were minimal. The cracked specimen was not sufficiently wide to obtain valid toughness values at room temperature.

Biaxial Properties

Typical stress-strain curves for the two alloys in a 1 to 2 stress field at the three test temperatures are shown in figure 7. At 20^o and 77^o K, the Ti-4Al-0.20 alloy cylinders generally failed immediately adjacent to the weld reinforcement. At 20^o K failure occurred before the 0.2 percent offset strain was reached. However, if the data

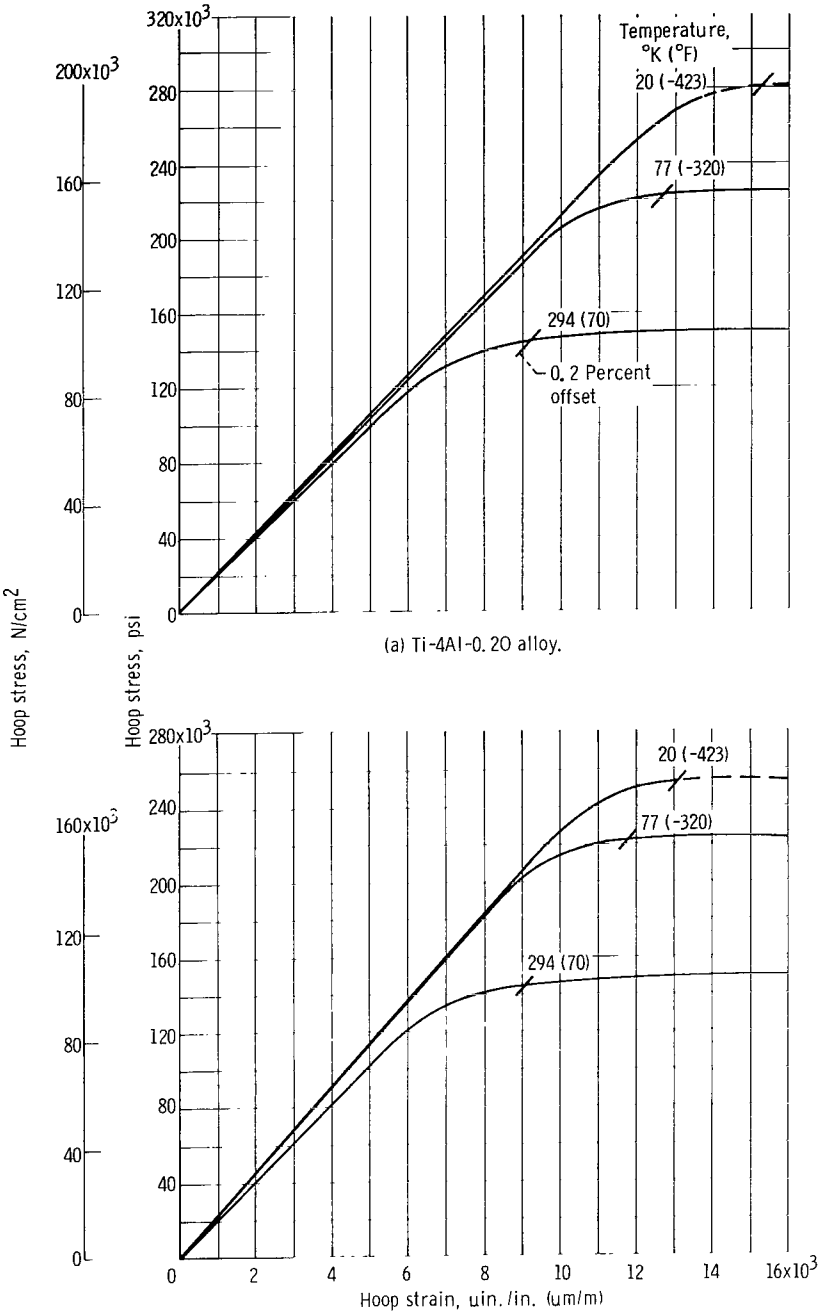

(a) Ti-4Al-0.2O alloy.

(b) Ti-5Al-2.5Sn ELI alloy.

Figure 7. - Typical stress-strain curves in 1 to 2 stress field.

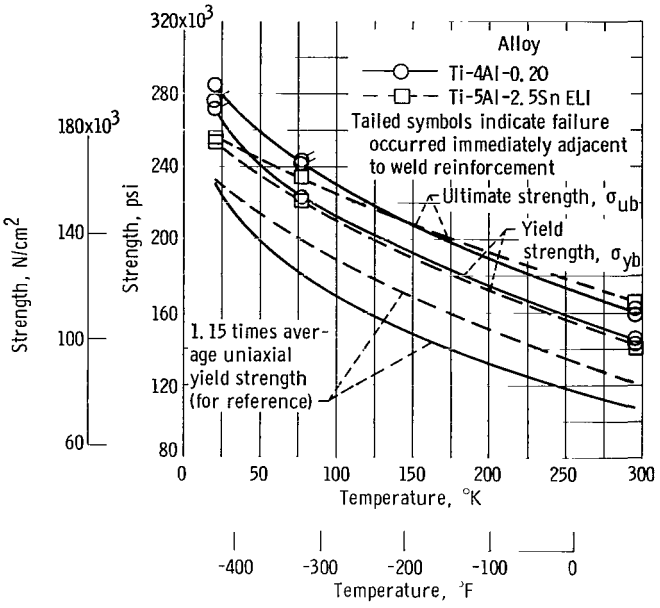

Figure 8. - Biaxial yield and ultimate strength of Ti-4Al-0.20 and Ti-5Al-2.5Sn ELI sheet in a 1 to 2 stress field as function of test temperature.

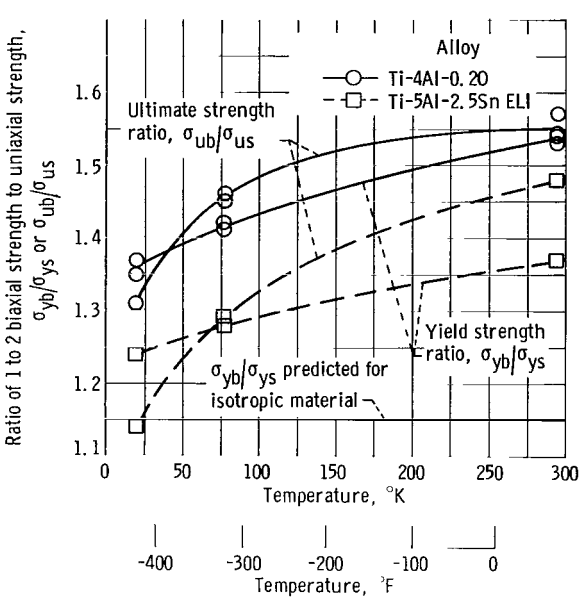

Figure 9. - Ratio of 1 to 2 biaxial strength to uniaxial strength of Ti-4Al-0.20 and Ti-5Al-2.5Sn ELI sheet as function of test temperature.

are extrapolated (fig. 7(a)) to the 0.2 percent offset strain, a yield strength of about 280 000 psi (190 000 N/cm^2) is indicated. The single Ti-4Al-0.20 alloy cylinder tested at 20° K that failed away from the weld reinforcement showed that the material was capable of developing this stress. For the cylinders that failed adjacent to the weld reinforcement before 0.2 percent offset strain was reached, the stress at burst can be considered to be a conservative estimate of the yield strength.

In figure 8, the biaxial yield and ultimate strengths are plotted as a function of test temperature for both alloys. To indicate the increase in yield strength predicted for an isotropic material, 1.15 times the average uniaxial yield strength is also included in figure 8. Individual test results are tabulated in table III.

Yield strength. - Both alloys developed biaxial yield strengths substantially greater than those predicted for isotropic materials. As figure 9 shows, strengthening ranged from 1.24 to 1.53 times the uniaxial yield strength. Strengthening was greater for the Ti-4Al-0.20 alloy at all temperatures investigated. Consequently, although the Ti-4Al-0.20 alloy had lower uniaxial yield strengths than the Ti-5Al-2.5Sn ELI alloy at the three test temperatures, the biaxial yield strengths for both alloys at 77° and 294° K were nearly identical. At 20° K, the biaxial yield strength of the Ti-4Al-0.20 alloy was about 9 percent greater than that of the Ti-5Al-2.5Sn ELI alloy. For both alloys, the strengthening effect of texture decreased as temperature decreased.

The experimental results were used to compute values of the strain ratio R from equation (1) in order to estimate the yield strengths of the two alloys in other stress

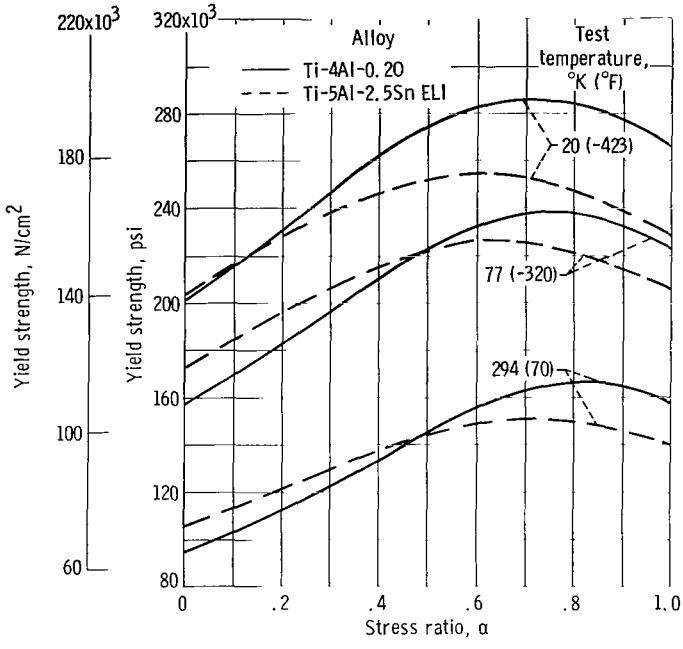

Figure 10. - Projected yield strengths for Ti-4Al-0.20 and Ti-5Al-2.5Sn ELI in tension-tension biaxial stress fields.

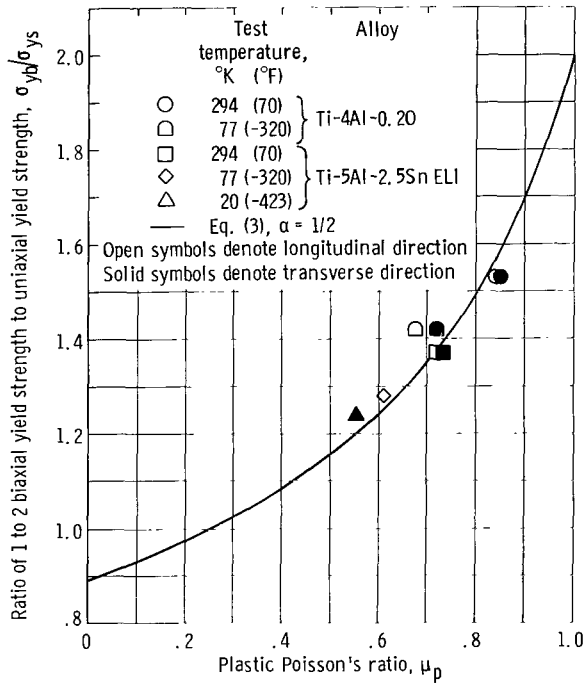

Figure 11. - Correlation of texture strengthening in a 1 to 2 stress field with plastic Poisson's ratio.

fields. These values are tabulated in table IV. The computed values of R were then used in equation (1) to calculate yield strengths in other biaxial stress fields. These projected yield strengths are shown in figure 10. At all three test temperatures, the yield strengths of the Ti-4Al-0.2O alloy are greater than those of the Ti-5Al-2.5Sn ELI alloy for stress ratios greater than 1/2. A stress field of particular interest is the 1 to 1 field (stress ratio, 1) which occurs in a pressurized spherical shell. For this case, the yield strengths projected for the Ti-4Al-0.2O alloy exceed those projected for the Ti-5Al-2.5Sn ELI alloy by 16, 9, and 13 percent at 20°, 77°, and 294° K, respectively. It is emphasized that these are projected strengths which have not been experimentally verified.

Equation (3) indicates that it should be possible to predict biaxial strengthening in a sheet material from its plastic Poisson's ratio. Values of μ_p were obtained experimentally in order to verify equation (3). At room temperature, the average value of μ_p for the Ti-4Al-0.2O alloy was 0.845 (R = 5.45 from eq. (2)). This value compares with an average of 0.772 obtained by Babel and Corn (ref. 15) for the same heat of material but for a thickness of 0.057 inch (0.145 cm). Reduction of thickness from 0.057 inch (0.145 cm) to 0.020 inch (0.051 cm) appears to intensify texture. For the Ti-5Al-2.5Sn ELI alloy μ_p was 0.732 (R = 2.73) at room temperature. In figure 11, the average σ_{yb}/σ_{ys} obtained from pressure vessel tests are plotted as a function of the values of μ_p obtained in this program, where σ_{yb} is the 1 to 2 biaxial yield strength. In table IV, values are tabulated of average σ_{yb}/σ_{ys}, μ_p obtained experimentally, and R obtained from σ_{yb}/σ_{ys} using equation (1). Also included in this table are R and σ_{yb}/σ_{ys} predicted by the average μ_p from equations (2) and (3), respectively.

In general the use of μ_p to predict strengthening resulted in values close to those obtained experimentally. At 294° K use of μ_p resulted in predictions of strengthening greater than that which actually occurred, while at 20° and 77° K the predictions were low. The greatest difference occurred with the Ti-4Al-0.2O alloy at 77° K where use of μ_p resulted in a prediction 7 percent less than was obtained from pressure vessel tests. The relation between μ_p and biaxial strengthening provides a relatively simple and economical means of investigating the possibility of variation in texture strengthening within a sheet, from sheet to sheet of the same heat, and from heat to heat of the same alloy.

Ultimate strength. - Substantial increases in 1 to 2 biaxial ultimate strength were also demonstrated by both alloys. In cases where failure occurred adjacent to the weld reinforcement, the longitudinal stress at the failure location was probably less than one-half the hoop stress ($\alpha < 1/2$), and the values shown in figure 8 are probably lower than those which would be obtained in a true 1 to 2 stress field. Examination of figure 9 shows that the ratio of biaxial to uniaxial ultimate strength σ_{ub}/σ_{us} exceeds the ratio of biaxial to uniaxial yield strength σ_{yb}/σ_{ys} in some cases, while in other cases it is

less than σ_{yb}/σ_{ys}. The greatest difference occurred with the Ti-5Al-2.5Sn ELI alloy at room temperature, where $\sigma_{yb}/\sigma_{ys} = 1.37$ and $\sigma_{ub}/\sigma_{us} = 1.48$. For the same alloy and thickness (but a different heat), Babel, et al. (ref. 6) obtained values of 1.27 and 1.54 for σ_{yb}/σ_{ys} and σ_{ub}/σ_{us}, respectively. This result shows twice the percentage increase in biaxial ultimate strength compared with the increase in biaxial yield strength. The Douglas biaxial specimen used by Babel is a 4-inch- (10.1-cm-) diameter cylinder 0.050 inch (0.127 cm) thick with a chemically milled 0.020-inch- (0.051-cm-) thick "window" for the test section. The higher biaxial ultimate strengths obtained with the Douglas specimen may have resulted from the thinner test section being restrained by the thicker section after yielding had occurred in the window. This condition would result in higher burst pressures.

At present there is no way to predict biaxial burst strength from uniaxial properties. Some suggest associating a value of R with biaxial ultimate strength, but this procedure requires biaxial tests. It may be possible to relate the biaxial fracture envelope to the results of uniaxial compression thickness tests. The method for predicting biaxial fracture strength being considered at Lewis is based on a tensile instability analysis that takes anisotropy into account.

Notch strength. - It is demonstrated in reference 16 that the behavior of a cylindrical pressure vessel in the presence of a longitudinal through crack can be correlated with the uniaxial behavior by

$$\sigma_{hc} = \frac{K_c}{\sqrt{\pi a_c + \frac{1}{2}\frac{K_c^2}{\sigma_{yb}^2}\left(1 + C\frac{a_c}{r}\right)}} \tag{4a}$$

based on the critical half-crack length a_c, or by

$$\sigma_{hc} = \frac{K_{cn}}{\sqrt{\pi a_o + \frac{1}{2}\frac{K_{cn}^2}{\sigma_{yb}^2}\left(1 + C\frac{a_o}{r}\right)}} \tag{4b}$$

based on the initial half-crack length a_o; where σ_{hc} is the critical hoop fracture stress in the cylinder, K_c is the fracture toughness (based on critical crack length), K_{cn} is the nominal fracture toughness (based on initial crack length), σ_{yb} is the 1 to 2 biaxial yield strength, r is the cylinder radius, and C is a dimensionless bulge coef-

ficient. The term $1 + C(a_c/r)$ (or $1 + C(a_o/r)$) takes into account the increase in stress intensity at the crack tips caused by bulging in a pressurized cylinder.

The results of the burst tests of through-cracked cylinders based on initial crack length and on critical crack length are shown in figure 12. Individual test results are presented in table V. The values of C used to draw the curves in figure 12 were obtained for each material and temperature by averaging the values of C computed from equation (4) for the individual data points. A weighted average described in reference (16) was used for both alloys. This average takes into account the greater sensitivity of C to an error in fracture toughness or critical crack length for cylinders with shorter crack lengths; consequently, it weighs the longer crack lengths more heavily. As a_c (or a_o) approaches zero, the critical hoop stress predicted by equation (4) exceeds the actual biaxial burst strength (i.e., at $a_c = 0$ ($a_o = 0$), $\sigma_{hc} = \sqrt{2}\,\sigma_{yb}$). Therefore, all curves in figure 12 are terminated at the biaxial ultimate strength in the region of small crack lengths.

For all the crack lengths tested, the Ti-4Al-0.2O alloy exhibited greater notch sensitivity than did the Ti-5Al-2.5Sn ELI alloy. Because the uniaxial fracture toughness properties of the two alloys are about the same, the relatively large difference in the biaxial results for longer cracks was not expected. A portion of the difference can be attributed to a higher residual stress condition in the Ti-4Al-0.2O alloy cylinders caused by using a lower temperature and a shorter time in the stress relief of these cylinders. By measuring the radius to which the cylinders opened when slit longitudinally, it was calculated that approximately 25 percent of the residual stress due to forming was still present in the Ti-4Al-0.2O alloy cylinders; this compares with less than 10 percent in the Ti-5Al-2.5Sn ELI alloy cylinders. However, this known difference in residual stress might not account completely for the difference in the biaxial notch strengths. The results of tests of non-stress-relieved Ti-5Al-2.5Sn ELI alloy cylinders (unpublished data obtained by F. D. Calfo of Lewis) are also plotted in figures 12(a) and (b) for tests at 77° and 20° K, respectively. The reduction in hoop fracture strength, with 100 percent of the residual stress due to forming remaining, was not great enough to cause the non-stress-relieved Ti-5Al-2.5Sn ELI alloy cylinders to fail at stresses less than those at which the Ti-4Al-0.2O alloy cylinders failed. However, for small cracks (0.1 in. (0.25 cm) or less), it is likely that the difference between the notch strengths of the two alloys will be small.

Biaxial strength in design. - Some of the ramifications of using biaxial yield strength in design became apparent during the biaxial test phase of this program. As stated earlier in this section, the Ti-4Al-0.2O alloy cylinders, at 20° and 77° K, frequently failed immediately adjacent to the weld reinforcement. The application of the reinforcement restrained the cylinders longitudinally in the vicinity of the weld. The stress ratio in the material immediately adjacent to the reinforcement was less than 1/2, with the

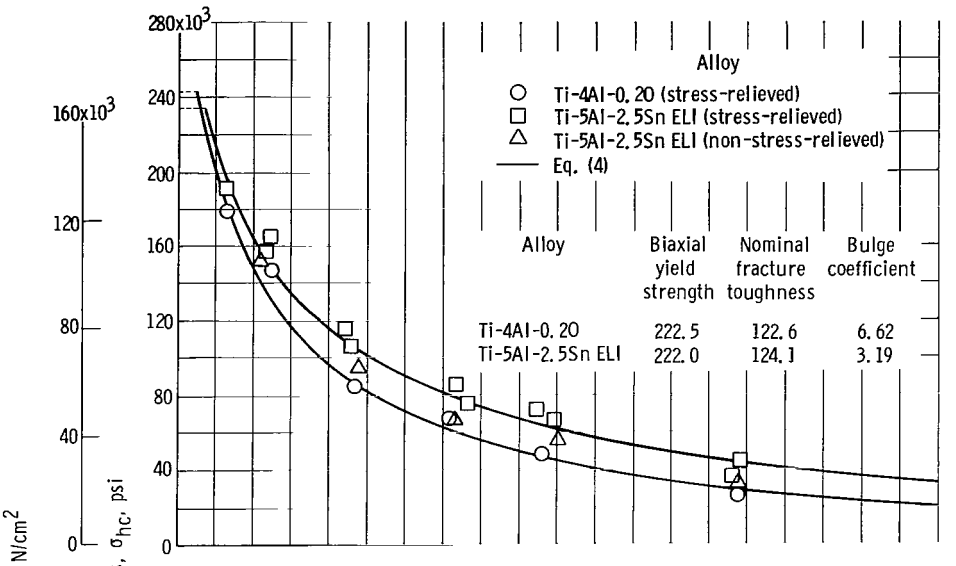

(a) Test at 77° K (-320° F), based on initial crack length.

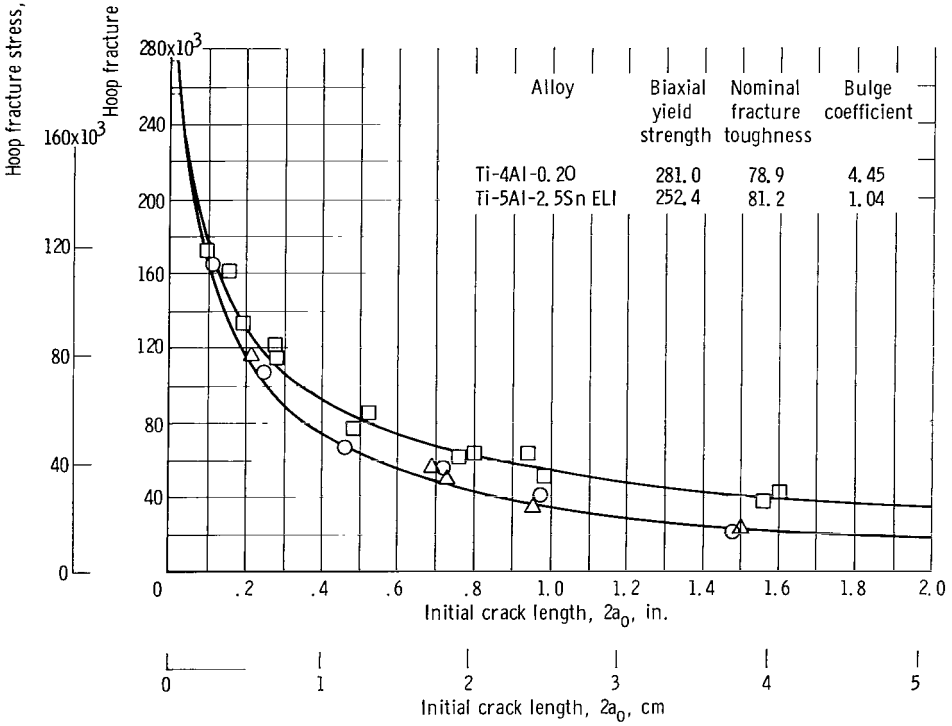

(b) Test at 20° K (-423° F), based on initial crack length.

Figure 12. - Strength of cracked titanium cylinders.

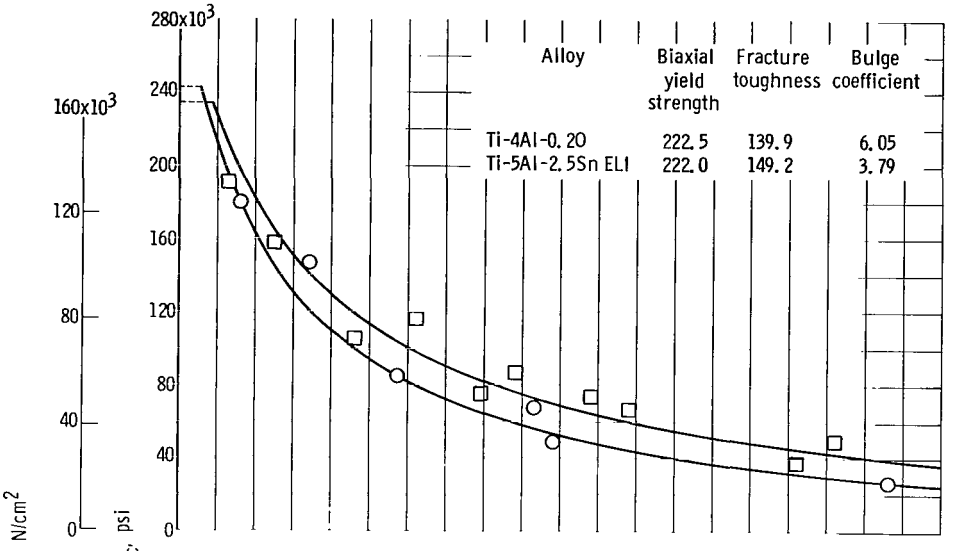

(c) Test at 77° K (-320° F), based on critical crack length.

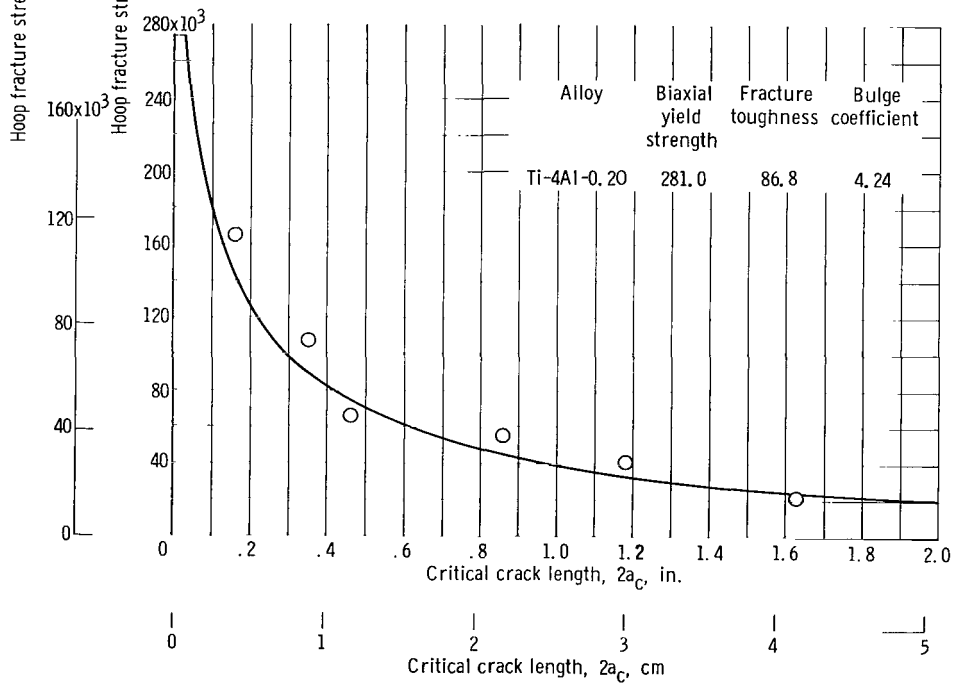

(d) Test at 20° K (-423° F), based on critical crack length.

Figure 12. - Concluded.

exact value depending on the thickness of the reinforcement. As shown in figure 10, the Ti-4Al-0.2O alloy strength is quite sensitive to stress ratio. This sensitivity to stress ratio combined with the residual stress in these cylinders probably reduced the strength adjacent to the reinforcement sufficiently to cause failure there at cryogenic temperatures. At room temperature, the material had sufficient ductility to overcome the dual effect of residual stress and a less advantageous stress ratio. The single cryogenically tested Ti-4Al-0.2O alloy cylinder that failed away from the weld reinforcement had the reinforcement built up gradually in three increments. Each incremental layer was 0.004 inch (0.010 cm) thick and was 1/2 inch (1.3 cm) narrower than the preceding layer. The sensitivity of biaxial strength to stress ratio must be kept in mind by the designer, and special care should be exercised in areas of discontinuity.

Uniaxial And Biaxial Weld Strength

The uniaxial and 1 to 2 biaxial weld strengths of the Ti-4Al-0.2O alloy are shown in figure 13 as a function of test temperature. The biaxial weld strength of Ti-5Al-2.5Sn ELI at 77° K is included in this figure. Individual test results are given in table VI. In all cases, the strengths of the uniaxial Ti-4Al-0.2O alloy weld specimens were greater than those of the parent metal. Investigation of uniaxial weld strength of the Ti-5Al-2.5Sn ELI alloy at 20° and 294° K shows it to be close to that of the parent metal (refs. 14 and 17).

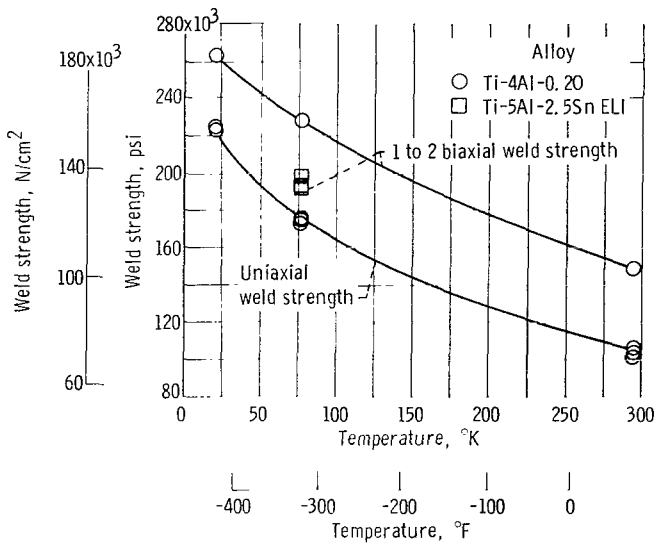

Figure 13. - Uniaxial and 1 to 2 biaxial weld strength of Ti-4Al-0.2O and Ti-5Al-2.5Sn ELI sheet as function of test temperature.

Contrary to the uniaxial behavior, the biaxial weld strength was in all cases less than the biaxial ultimate strength of the parent metal. However, the weld strengths of the Ti-4Al-0.2O alloy at 77° and 294° K exceeded the biaxial yield strength. In all cases, the fracture occurred immediately adjacent to the weld bead. Biaxial weld data for the Ti-5Al-2.5Sn ELI alloy were obtained only at 77° K. While the parent biaxial yield strengths of the two alloys at this temperature were nearly identical, the biaxial weld strength of the Ti-4Al-0.2O alloy was about 17 percent greater than that of the Ti-5Al-2.5Sn ELI alloy. The biaxial weld data obtained in this program are limited in number. If subsequent tests produce the same results, the Ti-4Al-0.2O alloy may have a considerable advantage over the Ti-5Al-2.5Sn ELI alloy in flaw-free, weld-critical, biaxially-stressed structures.

SUMMARY AND CONCLUSIONS

Tests of Ti-4Al-0.2O and Ti-5Al-2.5Sn ELI alloy pressure vessels fabricated from 0.020-inch- (0.051-cm-) thick sheet resulted in yield and ultimate strengths in a 1 to 2 stress field that in some cases were more than 50 percent greater than those obtained uniaxially. With both alloys, the strengthening effect of texture decreased as temperature decreased. On the basis of biaxial yield and ultimate strengths, the Ti-4Al-0.2O alloy with a room-temperature plastic Poisson's ratio of 0.845 was generally superior to the Ti-5Al-2.5Sn ELI alloy (room-temperature plastic Poisson's ratio, 0.732) at 20°, 77°, and 294° K, especially when the experimental yield-strength data were projected for stress ratios greater than 1/2. For the limited data available, the Ti-4Al-0.2O alloy also exhibited superior weld strength. However, the Ti-5Al-2.5Sn ELI alloy developed greater biaxial notch strength for through cracks longer than about 0.10 inch (0.25 cm).

In designs based on biaxial strength, care must be taken to ensure that the stress field is as anticipated and not changed to a less advantageous one (e.g., in the presence of doublers, reinforcements, etc.).

Plastic Poisson's ratio obtained from a uniaxial tension test can be used to characterize the degree of texture in sheet material and to provide a means for predicting biaxial strengthening.

Lewis Research Center,
National Aeronautics and Space Administration,
Cleveland, Ohio, October 13, 1967,
124-08-08-19-22.

REFERENCES

1. Backofen, W. A.; Hosford, W. F., Jr.; and Burke, J. J.: Texture Hardening. Trans. ASM, vol. 55, no. 1, Mar. 1962, pp. 264-267.

2. Larson, Frank R.: Anisotropy of Titanium Sheet in Uniaxial Tension. Trans. ASM, vol. 57, no. 3, Sept. 1964, pp. 620-631.

3. Hatch, A. J.: Texture Strengthening of Titanium Alloys. Trans. AIME, vol. 233, no. 1, Jan. 1965, pp. 44-50.

4. Larson, Frank R.: Textures in Titanium Sheet and Its Effects on Plastic Flow Properties. Rep. No. AMRA-TR-65-24, Army Materials Research Agency, Oct. 1965. (Available from DDC as AD-626410.)

5. Sliney, Joseph L.; Corrigan, Donald A.; and Schmid, Frederick: Preliminary Report on the Biaxial Tensile Behavior of Anisotropic Sheet Materials. Rep. No. AMRA-TR-63-11, Army Materials Research Agency, Aug. 1963. (Available from DDC as AD-421815.)

6. Babel, Henry W.; Eitman, David A.; and McIver, Robert W.: The Biaxial Strengthening of Textured Titanium. Paper No. 66-Met-6, ASME, Apr. 1966.

7. McHargue, Carl J.; Adair, Sam E., Jr.; and Hammond, Joseph P.: Effects of Solid Solution Alloying on the Cold-Rolled Texture of Titanium. Trans. AIME, vol. 197, no. 9, Sept. 1953, pp. 1199-1203.

8. Broadwell, R. G.; and Wood, R. A.: Titanium Alloys for Cryogenic Service. Mat. Res. and Standards, vol. 4, no. 10, Oct. 1964, pp. 549-554.

9. Hill, R.: A Theory of the Yielding and Plastic Flow of Anisotropic Metals. Proc. Roy. Soc. London. Ser. A, vol. 193, no. 1033, May 27, 1948, pp. 281-297.

10. Sullivan, Timothy L.; and Orange, Thomas W.: Continuity Gage Measurement of Crack Growth on Flat and Curved Surfaces at Cryogenic Temperatures. NASA TN D-3747, 1966.

11. Calvert, Howard F.; and Kemp, Richard H.: Determination of Pressure Vessel Strengths at -423° F as Influenced by Notches of Various Radii. Paper No. 520B, SAE, Apr. 1962.

12. Taylor, Abraham: X-ray Metallography. John Wiley & Sons, Inc., 1961.

13. ASTM Special Committee on Fracture Toughness Testing of High-Strength Metallic Materials. Fracture Testing of High-Strength Sheet Materials. Bull. No. 243, ASTM, Jan. 1960, pp. 29-40.

14. Shannon, J. L., Jr.; and Brown, W. F., Jr.: Effects of Several Production and Fabrication Variables on Sharp Notch Properties of 5Al-2.5Sn Titanium Alloy Sheet at Liquid Hydrogen Temperature. Proc. ASTM, vol. 63, 1963, pp. 809-829.

15. Babel, H. W.; and Corn, D. L.: A Comparison of Methods for Correlating Texturing with the Biaxial Strengths of Titanium Alloys. Metals Eng. Quarterly, vol. 7, no. 1, Feb. 1967, pp. 45-53.

16. Anderson, Robert B.; and Sullivan, Timothy L.: Fracture Mechanics of Through-Cracked Cylindrical Pressure Vessels. NASA TN D-3252, 1966.

17. Christian, J. L.; Hurlich, A.; Chafey, J. E.; and Watson, J. F.: Effects of Impurity Elements and Cold Rolling on the Mechanical Properties of Titanium-5Al-2.5Sn Alloy at Room and Cryogenic Temperatures. Proc. ASTM, vol. 63, 1963, pp. 578-597.

TABLE I. - UNIAXIAL SMOOTH PROPERTIES

Temperature		Direction	0.2 Percent yield strength		Ultimate strength		Modulus of elasticity		Elongation in 2 in. (5 cm), percent
°K	°F	(a)	psi	N/cm^2	psi	N/cm^2	psi	N/cm^2	
				Ti-4Al-0.2O					
20	-423	L	200.0×10^3	137.8×10^3	218.7×10^3	150.7×10^3	16.9×10^6	11.6×10^6	5.5
			198.9	137.0	216.4	149.1	17.3	11.9	4.5
			199.4	137.4	215.8	148.7	17.0	11.7	5.0
		Average	199.4×10^3	137.4×10^3	217.0×10^3	149.5×10^3	17.1×10^6	11.8×10^6	5.0
		T	203.6×10^3	140.3×10^3	216.8×10^3	149.4×10^3	16.9×10^6	11.6×10^6	2.5
			202.3	139.4	217.1	149.6	16.9	11.6	8.0
			202.4	139.5	216.8	149.4	17.5	12.1	5.5
		Average	202.8×10^3	139.7×10^3	216.9×10^3	149.4×10^3	17.1×10^6	11.8×10^6	5.3
77	-320	L	156.7×10^3	108.0×10^3	167.2×10^3	115.2×10^3	17.3×10^6	11.9×10^6	21.0
			156.9	108.1	165.9	114.2	17.3	11.9	19.0
			154.4	106.4	165.0	113.7	17.1	11.8	20.0
		Average	156.0×10^3	107.5×10^3	166.0×10^3	114.4×10^3	17.2×10^6	11.9×10^6	20.0
		T	158.2×10^3	109.0×10^3	166.5×10^3	114.7×10^3	17.4×10^6	12.0×10^6	17.5
			160.7	110.7	169.9	117.1	17.8	12.3	13.0
			155.6	107.2	164.8	113.5	17.6	12.1	18.0
		Average	158.2×10^3	109.0×10^3	167.1×10^3	115.1×10^3	17.6×10^6	12.1×10^6	16.2
294	70	L	95.8×10^3	66.0×10^3	105.4×10^3	72.6×10^3	16.7×10^6	11.5×10^6	20.0
			92.3	63.6	106.2	73.2	16.7	11.5	20.0
			93.3	64.3	102.3	70.5	16.5	11.4	20.0
		Average	93.8×10^3	64.6×10^3	104.6×10^3	72.1×10^3	16.6×10^6	11.5×10^6	20.0
		T	94.3×10^3	65.0×10^3	101.7×10^3	70.1×10^3	16.7×10^6	11.5×10^6	17.5
			94.8	65.3	106.4	73.3	16.8	11.6	16.5
			95.7	65.9	103.5	71.3	16.6	11.4	18.5
		Average	94.9×10^3	65.4×10^3	103.9×10^3	71.6×10^3	16.7×10^6	11.5×10^6	17.5
				Ti-5Al-2.5Sn ELI					
20	-423	L	203.7×10^3	140.3×10^3	224.2×10^3	154.5×10^3	17.8×10^6	12.3×10^6	(b)
			203.4	140.1	224.3	154.5	17.3	11.9	↓
			198.0	136.4	225.3	155.2	17.1	11.8	
			203.1	139.9	224.1	154.4	17.6	12.1	
			207.2	142.8	228.7	157.6	18.1	12.5	
			205.3	141.5	226.7	156.2	18.1	12.5	
		Average	203.5×10^3	140.2×10^3	225.6×10^3	155.4×10^3	17.7×10^6	12.2×10^6	(b)
		T	202.9×10^3	139.8×10^3	223.4×10^3	153.9×10^3	19.9×10^6	13.7×10^6	↓
			205.0	141.2	221.0	152.3	18.9	13.0	
			201.7	139.0	223.7	154.1	18.5	12.7	
		Average	203.2×10^3	140.0×10^3	222.7×10^3	153.4	19.1×10^6	13.2×10^6	(b)
77	-320	L	172.3	118.7	179.9	124.0	18.2	12.5	(b)
			170.6	117.5	177.9	122.6	18.1	12.5	↓
			174.6	120.3	182.8	125.9	17.8	12.3	
			173.3	119.4	180.8	124.6	18.2	12.5	
			173.0	119.2	179.9	124.0	18.2	12.5	
		Average	172.8×10^3	119.1×10^3	180.3×10^3	124.2×10^3	18.1×10^6	12.5×10^6	(b)
		T	173.8×10^3	119.7×10^3	180.8×10^3	124.6×10^3	18.1×10^6	12.5×10^6	(b)
			174.7	120.4	181.0	124.7	18.1	12.5	↓
			176.9	121.9	183.5	126.4	17.7	12.2	
			173.8	119.7	179.4	123.6	18.0	12.4	
		Average	174.8×10^3	120.4×10^3	181.2×10^3	124.8×10^3	18.0×10^6	12.4×10^6	(b)
294	70	L	104.4×10^3	71.9×10^3	109.9×10^3	75.7×10^3	16.4×10^6	11.3×10^6	(b)
			106.0	73.0	111.1	76.5	16.5	11.4	↓
			104.3	71.9	109.2	75.2	16.1	11.1	
			104.4	71.9	110.4	76.1	15.7	10.8	
			104.8	72.2	110.0	75.8	16.4	11.3	
			105.6	72.8	110.2	75.9	16.3	11.2	
		Average	104.9×10^3	72.3×10^3	110.1×10^3	75.9×10^3	16.2×10^6	11.2×10^6	(b)
		T	103.3×10^3	71.2×10^3	114.1×10^3	78.6×10^3	16.8×10^6	11.6×10^6	(b)
			106.1	73.1	111.3	76.7	16.5	11.4	↓
			106.5	73.4	111.5	76.8	16.1	11.1	
			106.4	73.3	111.1	76.5	16.7	11.5	
		Average	105.6×10^3	72.8×10^3	112.0×10^3	77.2×10^3	16.5×10^6	11.4×10^6	(b)

[a] L, longitudinal; T, transverse.
[b] Not measured.

TABLE II. - UNIAXIAL NOTCH PROPERTIES

Temperature		Direction	Thickness		Initial crack length		Critical crack length		Gross fracture stress		Notch strength		Nominal fracture toughness		Fracture toughness	
^{o}K	^{o}F	(a)	in.	cm	in.	cm	in.	cm	psi	N/cm^2	psi	N/cm^2	$psi\sqrt{in.}$	$(N/cm^2)\sqrt{cm}$	$psi\sqrt{in.}$	$(N/cm^2)\sqrt{cm}$
Ti-4Al-0.2O																
20	-423	L	0.0174	0.0442	1.007	2.558	1.22	3.10	58.0×10^3	40.0×10^3	87.3×10^3	60.1×10^3	78.8×10^3	86.7×10^3	89.5×10^3	98.4×10^3
			.0169	.0429	1.003	2.548	1.11	2.82	59.0	40.7	88.7	61.1	80.1	88.1	85.5	94.0
			.0170	.0432	1.004	2.550	1.16	2.95	57.3	39.5	86.2	59.4	77.7	85.5	85.3	93.8
		Average	------	------	-----	-----	----	----	58.1×10^3	40.0×10^3	87.4×10^3	60.2×10^3	78.9×10^3	86.8×10^3	86.8×10^3	95.5×10^3
		T	0.0169	0.0429	1.033	2.624	1.13	2.87	59.6×10^3	41.1×10^3	91.0×10^3	62.7×10^3	82.5×10^3	90.8×10^3	87.5×10^3	96.2×10^3
			.0167	.0424	1.007	2.558	1.12	2.85	58.2	40.1	87.6	60.4	79.2	87.1	84.8	93.3
			.0203	.0516	1.025	2.604	1.16	2.95	58.7	40.4	89.2	61.5	80.8	88.9	87.6	96.4
		Average	------	------	-----	-----	----	----	58.8×10^3	40.5×10^3	89.3×10^3	61.5×10^3	80.8×10^3	88.9×10^3	86.6×10^3	95.3×10^3
77	-320	L	0.0168	0.0427	1.012	2.570	1.18	3.00	83.9×10^3	57.8×10^3	126.7×10^3	87.3×10^3	124.8×10^3	137.3×10^3	140.5×10^3	154.6×10^3
			.0169	.0429	1.024	2.601	1.23	3.12	80.8	55.7	122.8	84.6	119.9	131.9	138.2	152.0
			.0169	.0429	1.017	2.583	1.21	3.07	82.8	57.0	125.1	86.2	123.2	135.5	141.0	155.1
		Average	------	------	-----	-----	----	----	82.5×10^3	56.8×10^3	124.9×10^3	86.1×10^3	122.6×10^3	134.9×10^3	139.9×10^3	153.9×10^3
		T	0.0169	0.0429	1.011	2.568	1.24	3.15	81.2×10^3	55.9×10^3	122.6×10^3	84.5×10^3	119.5×10^3	131.4×10^3	140.1×10^3	154.1×10^3
			.0167	.0424	1.021	2.593	1.26	3.20	81.3	56.0	123.2	84.9	120.7	132.8	142.5	156.8
			.0204	.0518	1.058	2.687	1.23	3.12	77.9	53.7	120.2	82.8	117.4	129.1	131.8	145.0
		Average	------	------	-----	-----	----	----	80.1×10^3	55.2×10^3	122.0×10^3	84.1×10^3	119.2×10^3	131.1×10^3	138.1×10^3	151.9×10^3
294	70	L	0.0169	0.0429	1.015	2.578	(b)	(b)	64.9×10^3	44.7×10^3	98.1×10^3	67.6×10^3	(c)	(c)	(c)	(c)
			.0169	.0429	1.025	2.604	(b)	(b)	65.4	45.1	99.3	68.4	(c)	(c)	(c)	(c)
			.0171	.0434	1.030	2.616	(b)	(b)	64.2	44.2	97.8	67.4	(c)	(c)	(c)	(c)
		Average	------	------	-----	-----	----	----	64.8×10^3	44.6×10^3	98.4×10^3	67.8×10^3	---------	---------	---------	---------
		T	0.0166	0.0422	1.010	2.565	(b)	(b)	65.5×10^3	45.1×10^3	98.7×10^3	68.0×10^3	(c)	(c)	(c)	(c)
			.0169	.0429	1.020	2.591	(b)	(b)	65.5	45.1	99.2	68.3	(c)	(c)	(c)	(c)
			.0171	.0523	1.060	2.692	(b)	(b)	64.3	44.3	99.5	68.6	(c)	(c)	(c)	(c)
		Average	------	------	-----	-----	----	----	65.1×10^3	44.9×10^3	99.1×10^3	68.3×10^3	---------	---------	---------	---------

									Ti-5Al-2.5Sn ELI						
20	-423	L	0.0187	0.0475	1.045	2.654	1.16	2.95	58.5×10^3	40.3×10^3	89.9×10^3	61.9×10^3	81.4×10^3	89.5×10^3	87.2×10^3	95.9×10^3
			.0194	.0493	1.030	2.616	1.21	3.07	59.4	40.9	90.5	62.4	82.0	90.2	91.2	100.3
			.0185	.0470	1.007	2.558	1.22	3.10	58.9	40.6	88.6	61.0	80.2	88.2	91.0	100.1
		Average	------	------	-----	-----	----	----	58.9×10^3	40.6×10^3	89.6×10^3	61.7×10^3	81.2×10^3	89.3×10^3	89.8×10^3	98.8×10^3
		T	0.0176	0.0447	1.031	2.619	1.23	3.12	61.6×10^3	42.4×10^3	93.9×10^3	64.7×10^3	85.3×10^3	93.8×10^3	96.0×10^3	105.6×10^3
			.0176	.0447	1.032	2.621	1.28	3.25	64.4	44.4	98.1	67.6	89.6	98.6	103.8	114.2
			.0177	.0450	1.011	2.568	1.21	3.07	65.7	45.3	99.2	68.3	90.2	99.2	101.7	111.9
		Average	------	------	-----	-----	----	----	63.9×10^3	44.0×10^3	97.1×10^3	66.9×10^3	88.4×10^3	97.2×10^3	100.5×10^3	110.6×10^3
77	-320	L	0.0183	0.0465	1.042	2.647	1.35	3.43	84.9×10^3	58.5×10^3	130.1×10^3	89.6×10^3	126.1×10^3	138.7×10^3	154.4×10^3	169.8×10^3
			.0181	.0460	1.029	2.614	1.30	3.30	82.6	56.9	125.8	86.7	120.9	133.0	145.8	160.4
			.0184	.0467	1.028	2.611	1.26	3.20	85.1	58.6	129.3	89.1	125.2	137.7	147.4	162.1
		Average	------	------	-----	-----	----	----	84.2×10^3	58.0×10^3	128.4×10^3	88.5×10^3	124.1×10^3	136.5×10^3	149.2×10^3	164.1×10^3
		T	0.0173	0.0439	1.012	2.570	(b)	(b)	87.9×10^3	60.6×10^3	132.8×10^3	91.5×10^3	128.6×10^3	141.5×10^3	---------	---------
			.0208	.0528	1.050	2.667	(b)	(b)	85.3	58.8	131.2	90.4	127.3	140.0	---------	---------
			.0208	.0528	1.010	2.565	(b)	(b)	88.0	60.6	132.7	91.4	128.6	141.5	---------	---------
		Average	------	------	-----	-----	----	----	87.1×10^3	60.0×10^3	132.2×10^3	91.1×10^3	128.2×10^3	141.0×10^3	---------	---------
294	70	L	0.0182	0.0462	1.040	2.642	(b)	(b)	70.2×10^3	48.4×10^3	107.4×10^3	74.0×10^3	(c)	(c)	(c)	(c)
			.0200	.0508	1.045	2.654	(b)	(b)	70.5	48.6	108.2	74.5	(c)	(c)	(c)	(c)
			.0187	.0475	1.027	2.609	(b)	(b)	69.2	47.7	105.2	72.5	(c)	(c)	(c)	(c)
		Average	------	------	-----	-----	----	----	70.0×10^3	48.2×10^3	106.9×10^3	73.7×10^3	---------	---------	---------	---------
		T	0.0191	0.0485	1.033	2.624	(b)	(b)	71.6×10^3	49.3×10^3	109.2×10^3	75.2×10^3	(c)	(c)	(c)	(c)
			.0196	.0498	1.025	2.604	(b)	(b)	70.8	48.8	107.5	74.1	(c)	(c)	(c)	(c)
			.0189	.0480	1.041	2.644	(b)	(b)	69.5	47.9	106.4	73.3	(c)	(c)	(c)	(c)
		Average	------	------	-----	-----	----	----	70.6×10^3	48.6×10^3	107.7×10^3	74.2×10^3	---------	---------	---------	---------

[a] L, longitudinal; T, transverse.

[b] Not measured.

[c] Cracked specimen not sufficiently wide for valid toughness measurement at room temperature.

TABLE III. - BIAXIAL SMOOTH PROPERTIES

Temperature		0.2 Percent yield strength		Ultimate strength	
^{o}K	^{o}F	psi	N/cm^2	psi	N/cm^2
Ti-4Al-0.2O					
20	-423	[a,b] 271.8×10^3	[a,b] 187.3×10^3	----------	----------
		[a,b] 276.2	[a,b] 190.3	----------	----------
		(c)	(c)	284.6×10^3	196.1×10^3
77	-320	222.0	153.0	[a] 243.5	[a] 167.8
		223.0	153.6	[a] 241.6	[a] 166.5
294	70	144.0	99.2	159.5	109.9
		145.2	100.0	163.4	112.6
Ti-5Al-2.5Sn ELI					
20	-423	252.4×10^3	173.9×10^3	256.0×10^3	176.4×10^3
77	-320	222.0	153.0	234.0	161.2
294	70	143.8	99.1	164.8	113.5

[a] Failed under or immediately adjacent to weld reinforcement.

[b] Failed before 0.2 percent offset strain was reached. Yield strength was based on burst pressure.

[c] Strain gages failed before yield point was reached.

TABLE IV. - SUMMARY OF UNIAXIAL AND BIAXIAL YIELD AND ULTIMATE PROPERTIES

Temperature		Average uniaxial yield strength, σ_{ys}		Average 1 to 2 biaxial yield strength, σ_{yb}		Ratio of biaxial to uniaxial yield strength, σ_{yb}/σ_{ys}	Strain ratio from eq. (1), R	Elastic Poisson's ratio, μ_e	Plastic Poisson's ratio, μ_p
^oK	^oF	psi	N/cm^2	psi	N/cm^2				
Ti-4Al-0.2O									
20	-423	201.1×10^3	138.6×10^3	[a]274.0×10^3	[a]188.8×10^3	1.36	2.49	(b)	(b)
77	-320	157.1	104.5	222.5	153.3	1.42	3.06	0.350	0.697
294	70	94.4	65.0	144.6	99.6	1.53	4.70	.395	.845
Ti-5Al-2.5Sn ELI									
20	-423	203.4×10^3	140.1×10^3	252.4×10^3	173.9×10^3	1.24	1.53	0.380	0.557
77	-320	173.8	119.7	222.0	153.0	1.28	1.83	.390	.617
294	70	105.3	72.6	143.8	99.1	1.37	2.55	.410	.732

Temperature		Strain ratio based on μ_p from eq. (2), R	Yield strength ratio based on μ_p from eq. (3) ($\alpha = 1/2$), σ_{yb}/σ_{ys}	Average uniaxial ultimate strength, σ_{us}		Average 1 to 2 biaxial ultimate strength, σ_{ub}		Ratio of biaxial to uniaxial ultimate strength, σ_{ub}/σ_{us}
^oK	^oF			psi	N/cm^2	psi	N/cm^2	
Ti-4Al-0.2O								
20	-423	----	----	217.0×10^3	149.5×10^3	284.6×10^3	196.1×10^3	1.31
77	-320	2.30	1.35	166.6	114.8	242.6	167.2	1.46
294	70	5.45	1.57	104.3	71.9	161.4	111.2	1.55
Ti-5Al-2.5Sn ELI								
20	-423	1.26	1.20	224.1×10^3	154.4×10^3	256.0×10^3	176.4×10^3	1.14
77	-320	1.61	1.26	180.8	124.6	234.0	161.2	1.29
294	70	2.73	1.39	111.1	76.5	164.8	113.5	1.48

[a]Based on burst pressure because 0.2 percent offset strain was not achieved.
[b]Not measured.

TABLE V. - BIAXIAL NOTCH PROPERTIES

Temperature		Thickness		Electrical discharge slot length		Initial crack length		Critical crack length		Critical hoop stress	
°K	°F	in.	cm	in.	cm	in.	cm	in.	cm	psi	N/cm^2
Ti-4Al-0.2O											
20	-423	0.0203	0.0516	0.05	0.13	0.110	0.279	0.16	0.41	164.2×10^3	113.1×10^3
		.0175	.0445	.15	.38	.247	.627	.35	.89	106.8	73.6
		.0198	.0503	.30	.76	.459	1.166	.46	1.17	65.9	45.4
		.0192	.0488	.55	1.40	.721	1.831	.86	2.18	55.2	38.0
		.0213	.0541	.80	2.03	.974	2.474	1.18	3.00	40.3	27.8
		.0174	.0442	1.30	3.30	1.477	3.752	1.63	4.14	20.7	14.3
77	-320	0.0169	0.0429	0.05	0.13	0.128	0.325	0.16	0.41	178.4×10^3	122.9×10^3
		.0208	.0528	.15	.38	.242	.615	.34	.86	146.3	100.8
		.0173	.0439	.30	.76	.466	1.184	.57	1.45	84.3	58.1
		.0198	.0503	.55	1.40	.715	1.816	.93	2.36	67.4	46.4
		.0174	.0442	.80	2.03	.961	2.441	.98	2.49	47.9	33.0
		.0203	.0516	1.30	3.30	1.473	3.741	1.86	4.72	25.9	17.8
Ti-5Al-2.5Sn ELI											
20	-423	0.0209	0.0531	0.05	0.13	0.093	0.236	(a)	(a)	171.5×10^3	118.2×10^3
		.0213	.0541	.10	.25	.155	.394			160.9	110.9
		.0213	.0541	.10	.25	.190	.483			133.3	91.8
		.0212	.0538	.20	.51	.277	.704			121.4	83.6
		.0202	.0513	.20	.51	.280	.711			114.2	78.7
		.0213	.0541	.40	1.02	.523	1.328			84.6	58.3
		.0217	.0551	.40	1.02	.482	1.224			76.0	52.4
		.0200	.0508	.70	1.78	.803	2.040			63.6	43.8
		.0214	.0544	.70	1.78	.762	1.935			61.5	42.4
		.0210	.0533	.90	2.29	.941	2.390			63.0	43.4
		.0213	.0541	.90	2.29	.985	2.502			51.6	35.6
		.0181	.0460	1.40	3.56	1.600	4.064			40.6	28.0
		.0211	.0536	1.40	3.56	1.560	3.962			37.7	26.0
77	-320	0.0204	0.0518	0.10	0.25	0.125	0.318	0.13	0.33	190.4×10^3	131.2×10^3
		.0211	.0536	.20	.51	.241	.612	(b)	(b)	164.9	113.6
		.0204	.0518	.20	.51	.229	.582	.25	.64	156.6	107.9
		.0205	.0521	.40	1.02	.440	1.118	.62	1.57	115.5	79.6
		.0204	.0518	.40	1.02	.453	1.151	.46	1.17	105.1	72.4
		.0201	.0511	.70	1.78	.733	1.862	.88	2.24	84.9	58.5
		.0175	.0445	.70	1.78	.765	1.943	.79	2.01	74.6	51.4
		.0206	.0523	.90	2.29	.946	2.403	1.08	2.74	71.8	49.5
		.0193	.0490	.90	2.29	.991	2.517	1.18	3.00	66.2	45.6
		.0175	.0445	1.40	3.56	1.480	3.759	1.72	4.37	44.1	30.4
		.0213	.0541	1.40	3.56	1.460	3.708	1.62	4.11	35.9	24.7

[a]No detectable slow crack growth occurred.

[b]Slow crack growth not measured.

TABLE VI. - UNIAXIAL AND BIAXIAL WELD PROPERTIES

Stress field	Temperature		Failure stress		Weld efficiency, percent
	^{o}K	^{o}F	psi	N/cm^2	
Ti-4Al-0.2O					
Uniaxial	20	-423	224.5×10^3	154.7×10^3	100.0
			223.8	154.2	
			228.8	157.6	
			227.0	156.4	
	77	-320	174.2	120.0	
			173.9	119.8	
			173.3	119.4	
			174.9	120.5	
	294	70	106.2	73.2	
			106.9	73.7	
			105.8	72.9	
			115.4	79.5	
Biaxial	20	-423	262.5×10^3	180.9×10^3	92.3
	77	-320	228.2	157.2	94.3
	294	70	149.3	102.9	92.4
Ti-5Al-2.5Sn ELI					
Biaxial	77	-320	192.6×10^3	132.7×10^3	82.3
			190.8	131.5	81.5
			197.3	135.9	84.3